8984–8991 *Nucleic Acids Research, 2011, Vol. 39, No. 20* *Published online 19 July 2011*
doi:10.1093/nar/gkr540

HIV-1 integrase inhibitor *T30177* forms a stacked dimeric G-quadruplex structure containing bulges

Vineeth Thachappilly Mukundan[1], Ngoc Quang Do[1,2] and Anh Tuân Phan[1,*]

[1]School of Physical and Mathematical Sciences and [2]School of Biological Sciences, Nanyang Technological University, Singapore

Received January 19, 2011; Revised June 10, 2011; Accepted June 13, 2011

ABSTRACT

***T30177* is a G-rich oligonucleotide with the sequence (GTGGTGGGTGGGTGGGT) which inhibits the HIV-1 integrase activity at nanomolar concentrations. Here we show that this DNA sequence forms in K^+ solution a dimeric G-quadruplex structure comprising a total of six G-tetrad layers through the stacking of two propeller-type parallel-stranded G-quadruplex subunits at their 5′-end. All twelve guanines in the sequence participate in the G-tetrad formation, despite the interruption in the first G-tract by a thymine, which forms a bulge between two adjacent G-tetrads. In this work, we also propose a simple analytical approach to stoichiometry determination using concentration-dependent melting curves.**

INTRODUTION

G-quadruplexes (1–5) are four-stranded structures formed by G-rich nucleic acid sequences. Formation of G-quadruplexes can affect a wide range of biological activities including telomere maintenance, gene regulation, transcription, DNA replication and repair (6). G-quadruplexes formed by synthetic oligonucleotides may possess anticancer (7–9) and anti-HIV (10–20) activity.

The basic unit of a G-quadruplex is a G-tetrad, a cyclic planar arrangement of four guanines linked by hydrogen bonds (21). The stability of a G-quadruplex depends on the stacking between different G-tetrads as well as electrostatic interaction mediated by cations, such as K^+ or Na^+, which are located at the center of the G-tetrad core. In most of the G-quadruplex structures reported so far, the G-tetrad core is formed by tracts of consecutive guanines (1–5). Formation of bulges has been observed in a G-quadruplex, where G-tracts are interrupted by non-guanine residues (22).

A series of G-rich DNA oligonucleotides (12–17) and their backbone-modified counterparts (11,12,23–25) have been reported to inhibit the activity of HIV-1 integrase (IN), an enzyme which is responsible for the integration of viral DNA into host genome (26). These include *T30695* (or *T30923*) with the sequence (GGGTGGGTG GGTGGGT) (14,15) and *T30177* (or *I100-15*) with the sequence (GTGGTGGGTGGGTGGGT) (11–13). These sequences were proposed to adopt a chair-type antiparallel-stranded G-quadruplex with two G-tetrads and three edgewise (T-G) loops (12,14,27). However, this proposed folding topology is at variance with the reported CD profile showing a positive peak at 260 nm (14,28), which is characteristic of a parallel-stranded G-quadruplex (29), and the mass spectrometry detection of a dimer for these sequences (28,30). Furthermore, a related G-rich oligonucleotide *93del* was determined by NMR to form an interlocked dimer comprising two parallel-stranded G-quadruplex subunits (17); sequences with GGG tracts separated by single-residue linkers were shown to form stable parallel-stranded G-quadruplexes in both experimental (31–37) and computational (33,38) studies.

In the accompanying paper (39), the *T30695* oligonucleotide with the sequence (GGGTGGGTGGGTGG GT) was determined to form a dimeric structure by the stacking of two propeller-type parallel-stranded G-quadruplex subunits, in which all G-tracts participate in the G-tetrad core formation. In this work, we investigate the structure of the G-rich oligonucleotide HIV-1 integrase inhibitor *T30177*, which differs from *T30695* by the presence of a T residue that interrupts the first G-tract. Our results showed that *T30177* forms a stacked dimeric G-quadruplex structure containing bulges. The knowledge of these structures might help us to uncover their inhibition mechanism against HIV-1 integrase. This work used a wide range of biophysical techniques including gel electrophoresis, CD, UV and NMR spectroscopy. We also propose a simple analytical approach to stoichiometry determination using concentration-dependent melting curves.

*To whom correspondence should be addressed. Tel: +65 6514 1915; Fax: +65 6794 1325 Email: phantuan@ntu.edu.sg

MATERIALS AND METHODS

Sample preparation

Unlabeled and site-specific labeled DNA oligonucleotides were chemically synthesized using products from Glen Research and Cambridge Isotope Laboratories. Samples were purified following Glen Research's protocol and then dialyzed successively against KCl solution and water. DNA oligonucleotides were dissolved in solution containing 70 mM potassium chloride and 20 mM potassium phosphate (pH 7.0). DNA concentration was expressed in strand molarity using a nearest-neighbor approximation for the absorption coefficients of the unfolded species (40).

NMR spectroscopy

NMR experiments were performed on 600 and 700 MHz NMR Bruker spectrometers. Guanine resonances were assigned by using site-specific ^{15}N and ^{2}H labeling (41,42) and through-bond correlations at natural abundance (43). Spectral assignments were completed by using NOESY, COSY, TOCSY and HSQC spectra (44). G-quadruplex folding topology was determined based on interproton distances obtained from NOESY experiments.

Gel electrophoresis

Electrophoresis experiment was performed at 120 V on native gels containing 20% polyacrylamide (Acrylamide: Bis-acrylamide = 37.5:1) in TBE buffer (89 mM Tris–borate, 2 mM EDTA, pH 8.3) supplemented with 3 mM KCl. Each sample contained 5 μg DNA. Gel was viewed by UV shadowing.

Circular dichroism

CD spectra were recorded on a JASCO-815 spectropolarimeter using 1 cm path-length quartz cuvette in a reaction volume of 600 μl at 20°C. Scans from 220 to 320 nm were performed with 200 nm/min, 1-nm pitch and 1-nm bandwidth. DNA concentration was 4–6 μM.

UV melting experiments

The stability of the G-quadruplex structure is measured in UV melting experiments conducted on a JASCO V-650 spectrophotometer. Absorbance at 295 nm was recorded as a function of temperature ranging from 30 to 90°C. The heating and cooling rates were 0.2°C/min. Experiments were performed with quartz cuvettes, with 1-cm path length. DNA concentration ranged from 0.5 to 200 μM. Solution contained 70 mM (or 30 mM) KCl and 20 mM potassium phosphate (pH 7.0).

RESULTS AND DISCUSSION

T30177 and *T30177-I11* form G-quadruplexes in K^+ solution

One-dimensional imino proton spectrum of *T30177* in K^+ solution (Figure 1a), similar to the one reported earlier (12), shows peaks in the range of 10.8–11.5 ppm, indicating the formation of a G-quadruplex. However, the heavy overlapping of these peaks makes further structural analysis difficult. This could be due to the structural symmetry, which arises from the repetitive nature of the sequence. We found that the DNA sequence with a single guanine-to-inosine substitution at position 11 showed greatly improved NMR spectra, and selected this sequence (henceforth designated as *T30177-I11*, Table 1) for further structural analysis. Similar spectral behavior was also observed (Supplementary Figure S1) for many different DNA sequences containing a single guanine-to-inosine substitution (Supplementary Table S1).

Imino proton spectrum of *T30177-I11* in K^+ solution (Figure 1b) shows peaks at 10.8–11.5 ppm corresponding to eleven guanine imino protons and an additional peak at

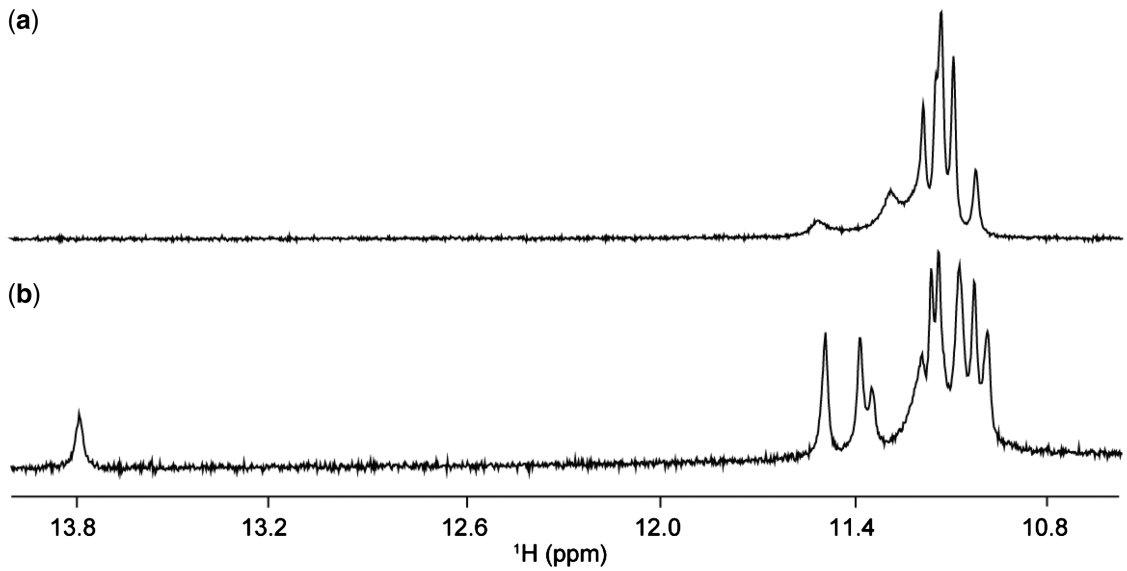

Figure 1. Imino proton NMR spectra of (**a**) *T30177* and (**b**) *T30177-I11* in K^+ solution at 25°C.

13.8 ppm corresponding to the imino proton of the inosine. This indicates the involvement of all 12 guanine and inosine bases in the G-tetrad formation, in contrast to only eight guanines for the previously proposed structure (12). Both *T30177* and *T30177-I11* give similar CD spectra (Figure 2) with a positive peak at 260 nm, which is characteristic of parallel-stranded G-quadruplexes (29).

A simple method for stoichiometry determination: *T30177-I11* forms a dimeric G-quadruplex

The temperature-driven folding/unfolding of *T30177-I11* was monitored by the UV absorbance at 295 nm (45) (Figures 3a and 4a). The 295-nm absorbance decreased with an increase of temperature, as typically observed for G-quadruplexes. The heating and cooling curves were almost superimposed indicating near equilibrium processes. The melting temperature (T_m) was dependent on DNA concentration: in ~100 mM K^+ solution, T_m increased from 68 to 76°C when the DNA concentration increased from 5 to 150 μM (Figure 3a); in ~60 mM K^+ solution, T_m increased from 63 to 73°C when the DNA concentration increased from 0.5 to 200 μM (Figure 4a). These results indicated the formation of a multimeric G-quadruplex.

Consider the equilibrium between a monomer and a multimer (*n*-mer):

$$n[C] \leftrightharpoons [C_n]$$

where $[C]$ and $[C_n]$ are the concentrations of the monomer and the *n*-mer respectively. The equilibrium concentrations of the two species are related via the dissociation constant (K_d) by:

$$K_d = [C]^n/[C_n]$$

The plot of the concentration of the *n*-mer against the concentration of the monomer in log scales should be a straight line with the slope *n* (44).

Here we propose a simple method to quantitatively analyze the concentration-dependent melting curves for stoichiometry determination. For a given temperature where the structural transition was observed (e.g. 70, 74 and 78°C, Figure 3a), concentrations of the folded and unfolded species were determined for each melting curve. The concentration of the folded species (*n*-mer) was

Table 1. DNA sequences used in this work

Name	Sequence (5′–3′)
T30177	G T GG T GGG T GGG T GGG T
T30177-I11	G T GG T GGG T G I G T GGG T
T30177-TT	TT G T GG T GGG T GGG T GGG T
T30177-I11-TT	TT G T GG T GGG T G I G T GGG T

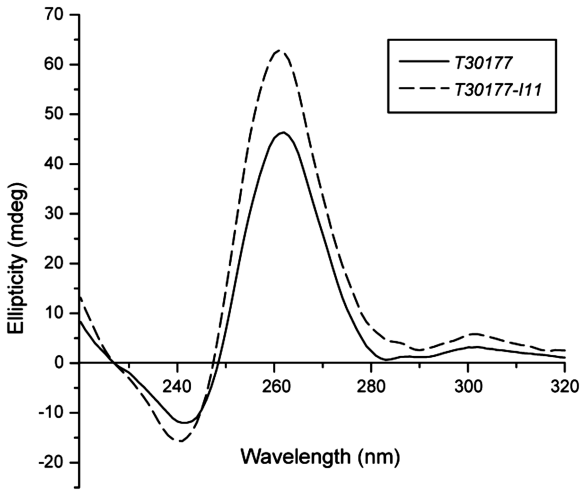

Figure 2. CD spectra of *T30177* and *T30177-I11* in K^+ solution at 20°C.

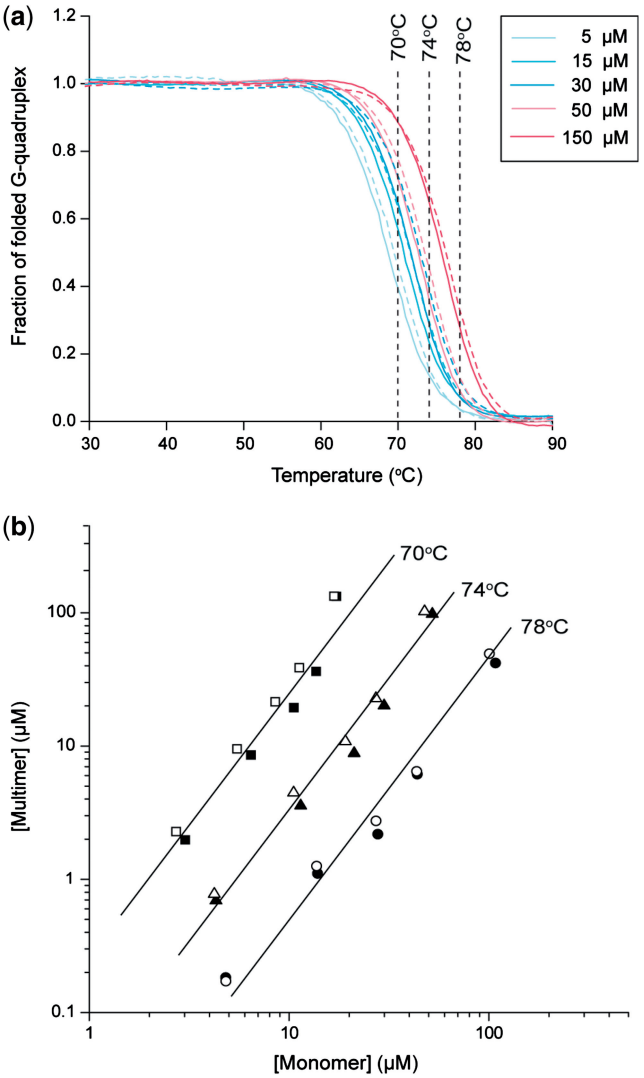

Figure 3. UV-melting data of *T30177-I11*. (**a**) Cooling and heating curves for a particular DNA concentration are shown in one color, with continuous and dashed lines respectively. Color codes are shown at the top right corner. (**b**) Plots of multimer concentrations against monomer concentrations at three different temperatures. Data were obtained from the melting curves in (a) with filled and open points corresponding to cooling and heating processes, respectively. Lines of slope 2 are drawn through the points. Samples contained 70 mM KCl and 20 mM potassium phosphate (pH 7.0).

plotted against the concentration of the unfolded species (monomer) in log scales (Figure 3b, Supplementary Figures S2, S3). The slope 2 would fit well the data points in ~100 mM K^+ solution at each temperature (Figure 3b) [the slope of the best fits ranged from 1.74 to 2.16 (Supplementary Figure S2)], indicating the formation of a dimer by *T30177-I11*. At 70°C, the dissociation constant K_d of this dimer is ~10 μM in this condition.

Quantitative analysis of concentration-dependent melting curves for stoichiometry determination has been previously reported (46,47). However, the proposed analysis was relatively complicated: the authors theoretically derived the analytical expression for the variation of T_m as a function of DNA concentration, i.e. using the interception points of a horizontal line at 0.5 with the melting curves; furthermore, measurements of the enthalpy (ΔH) associated with the transition were required for the stoichiometry determination. In contrast, our approach used interception points of vertical lines with the melting curves, and the analysis was quite simple. To our knowledge, this approach is being used here for the first time. We should note that the application of both approaches for quantitative analysis of concentration-dependent melting curves requires the assumption that these melting curves are equilibrium processes for a transition between two states: one folded and one unfolded. In practice, the equilibrium transitions can be achieved when the interconversion between these states is fast compared to the heating/cooling rate of the spectrometer.

The described analysis is based on the assumption that the observed changes in the UV absorbance reflect the multimer–monomer transition. However, in the present example (see structure below) the changes in the 295-nm UV absorbance only directly reflect the G-quadruplex unfolding, which in turn may depend on the dimer–monomer transition. In the given example, at very low DNA concentrations, monomeric intramolecular G-quadruplex can exist at a higher abundance. This can explain why the observed data points for low DNA concentrations (~1 μM) deviated from the slope 2 towards a shallower slope (Supplementary Figure S3).

Gel electrophoresis (Figure 5) showed that the migration of *T30177* and *T30177-I11* was similar to that of the interlocked dimeric G-quadruplex *93del* comprising six G-tetrad layers (17) and slower than that of a monomeric parallel-stranded propeller-type G-quadruplex *GTERT-60* with three tetrad layers (48), consistent with the formation of a dimeric G-quadruplex by *T30177* and *T30177-I11*. This result was corroborated by NMR data (discussion below).

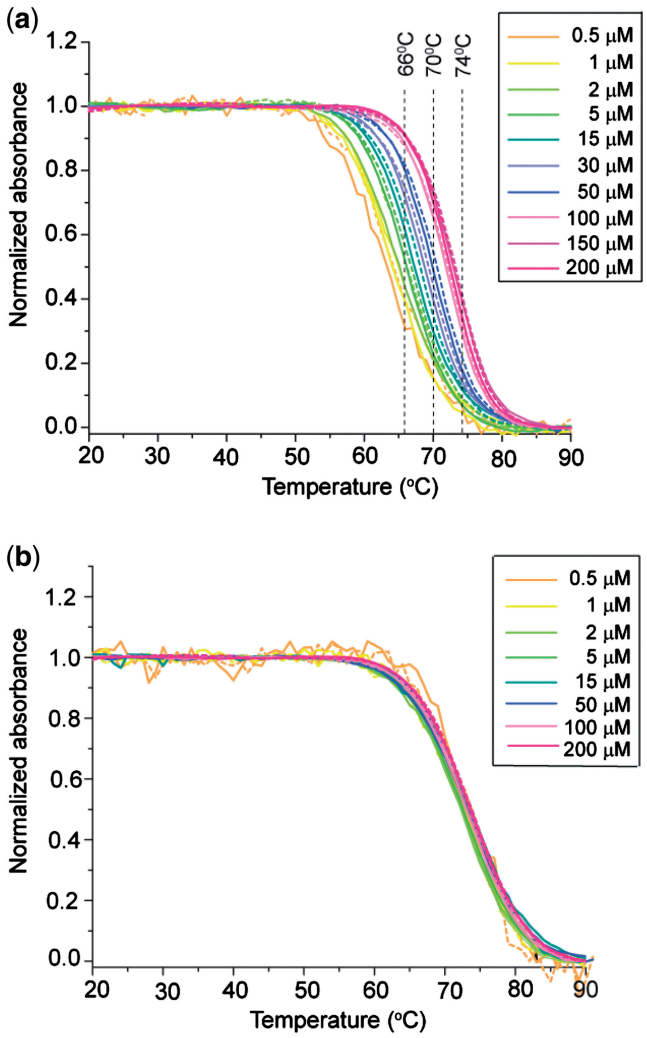

Figure 4. UV-melting data of (**a**) *T30177-I11* and (**b**) *T30177-I11-TT*. Cooling and heating curves for a particular DNA concentration are shown in one color, with continuous and dashed lines respectively. Color codes are shown at the top right corner. Samples contained 30 mM KCl and 20 mM potassium phosphate (pH 7.0).

NMR spectral assignments of *T30177-I11*

The downfield-shifted peak at 13.8 ppm was assigned to the imino proton of I11 (49). Guanine imino protons were unambiguously assigned to their respective positions in the sequence (Figure 6a) using the site-specific

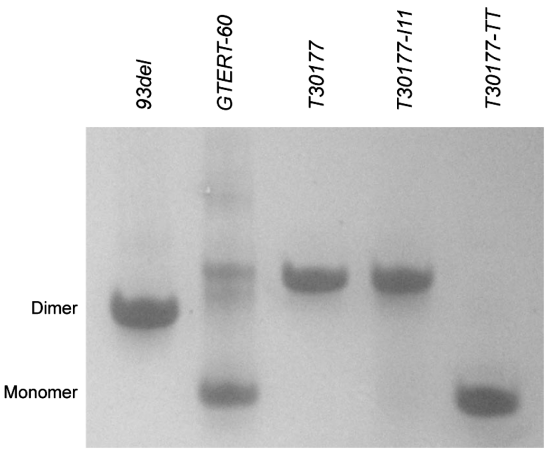

Figure 5. Gel electrophoresis analysis of *T30177* and its derivatives. Reference markers are *93del* (d[GGGTGGGAGGAGGGT]), an interlocked dimeric G-quadruplex (17) and *GTERT-60* (d[AGGGIAGGGGCTGGGAGGGC]), a monomeric propeller-type G-quadruplex (48). *T30177-TT* has two additional thymines at the 5′-end as compared to *T30177*.

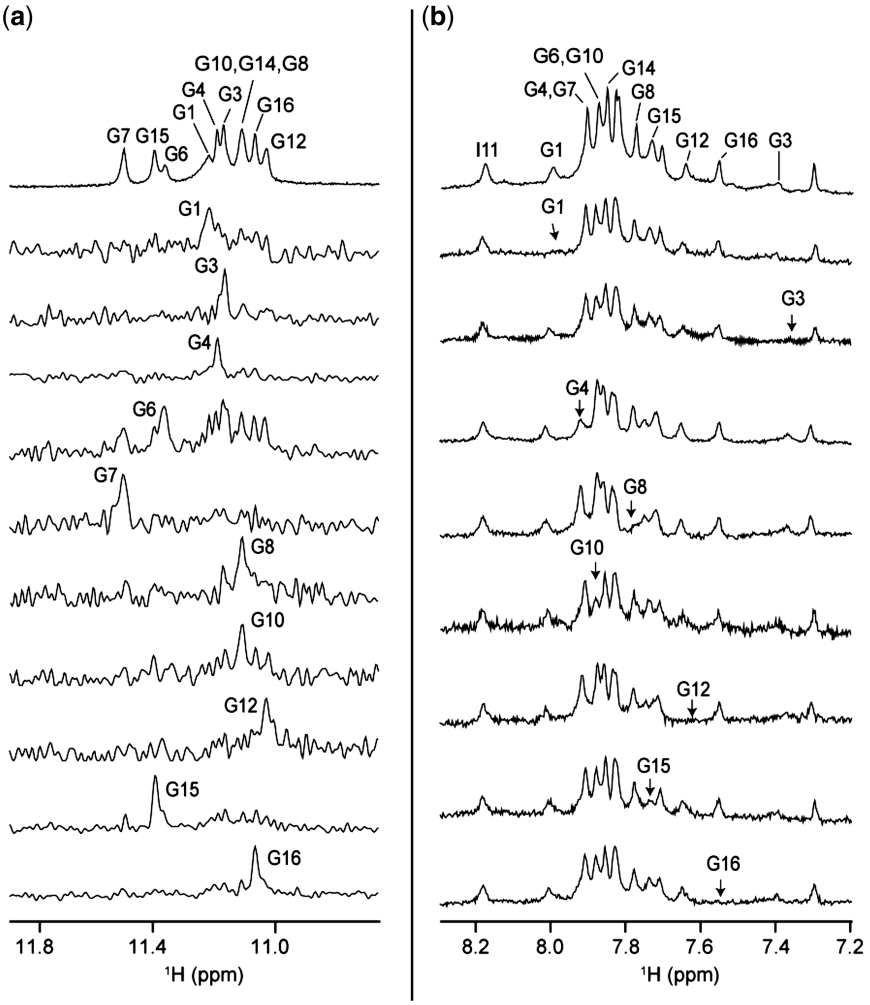

Figure 6. Resonance assignments of *T30177-I11* (**a**) Imino proton reference spectrum (top) with assignments indicated over the spectrum. Below are the ^{15}N-filtered spectra of samples, 2% ^{15}N labeled at the indicated position. (**b**) Aromatic reference spectrum (top) with assignments indicated over the spectrum. Below are the individual spectra, where the H8 protons are replaced by deuterium (^{2}H) at the indicated positions.

low-enrichment approach (41), in which one guanine at a time was ^{15}N-labeled at 2% (Supplementary Table S2). These assignments further confirmed that all guanines and inosine in the sequence participated in G-tetrad formation. Guanine H8 protons were assigned independently by site-specific ^{2}H substitutions at the H8 position of guanines one at a time (42,50) (Supplementary Table S2), which led to the disappearance of a single peak corresponding to the substituted guanine (Figure 6b).

Determination of folding topology: *T30177-I11* forms a stacked dimeric G-quadruplex

Using the complete assignments of imino (H1) and H8 protons, the G-tetrad alignments were determined from NOESY spectra based on the specific imino-H8 connectivities within a G-tetrad (Figure 7). For example, we observed NOE cross-peaks between G4(H1) and G8(H8), G8(H1) and G12(H8), G12(H1) and G16(H8), and G16(H1) and G4(H8), which established the formation of the (G4•G8•G12•G16) tetrad. In the same manner, we determined the arrangements of (G3•G7•I11•G15) and (G1•G6•G10•G14) tetrads (Figure 7c).

Figure 8 shows a dimeric folding topology for *T30177-I11* that satisfies the established alignments of the three G-tetrads. This is a dimeric G-quadruplex comprising two identical subunits of propeller-type parallel-stranded G-quadruplexes each containing three G-tetrad layers, three double-chain-reversal loops (T5, T9 and T13) and a bulge (T2). The two subunits are stacked at their 5′-end; there could be various isomers, where the two subunits are rotated with respect to each other about the common central helical axis. However, the broadening of peaks at the interface (see below) and the symmetric nature of the structure prevented us from definite determination of the orientation and the detailed structure of the stacking interface. The stacking mode shown in Figure 8 was proposed on the basis of the stacked dimeric structure of the homologue sequence *T30695* (39).

This folding topology is consistent with the results of a solvent-exchange experiment showing that imino

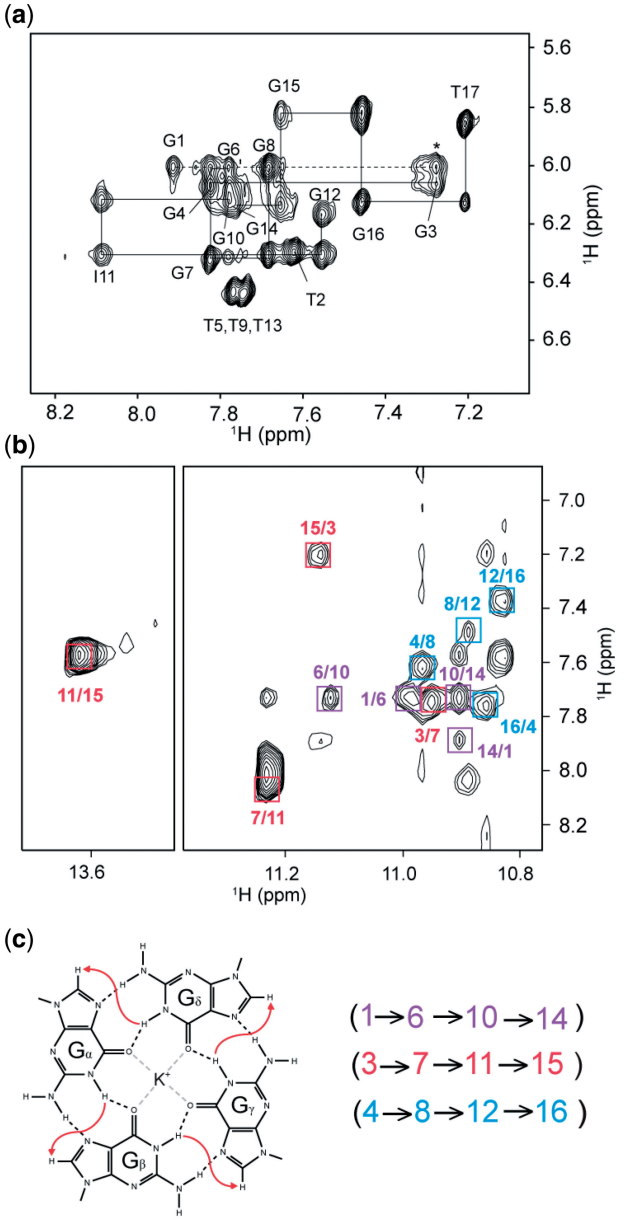

Figure 7. (**a**) NOESY spectrum (mixing time, 200 ms) showing the H8/H6-H1′ connectivity of *T30177-I11* in K^+ solution. The assignments and H8/6-H1′ NOE sequential connectivities are shown. Intra-residue cross-peaks are labeled with the corresponding residue numbers. NOE connectivity between G1 and G3 across the bulge T2 is indicated with a dashed line; The cross-peak between G1(H1′) and G3(H8) is labeled with an asterisk. (**b**) NOESY spectrum (mixing time, 200 ms) showing the imino-H8 connectivity around different G-tetrads. The characteristic guanine imino-H8 cross-peaks for G-tetrads are framed and labeled with the imino proton assignment in the first position and that of the H8 proton in the second position. The residues in different G-tetrads are indicated by different colors. (**c**) Specific imino-H8 connectivity pattern around a G_α•G_β•G_γ•G_δ tetrad indicated with arrows. Characteristic guanine imino-H8 NOE connectivities observed for G1•G6•G10•G14 (purple), G3•G7•I11•G15 (red), and G4•G8•G12•G16 (blue) tetrads.

protons belonging to the central (G3•G7•I11•G15) and the 5′-end (G1•G6•G10•G14) tetrads are the most protected (Figure 9). The glycosidic conformations of all residues are *anti*, as shown by the moderate intensities of

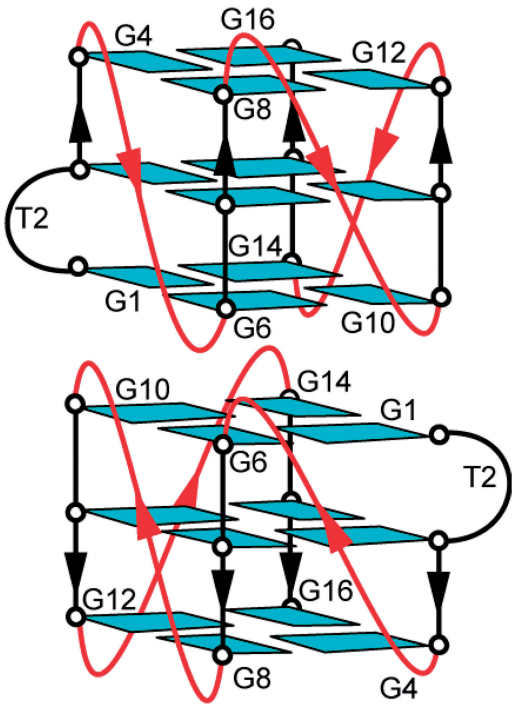

Figure 8. Schematic structure of the G-quadruplex adopted by *T30177-I11* in K^+ solution.

H1′-H8/6 NOE cross-peaks (Figure 7a), consistent with the formation of a parallel-stranded G-quadruplex (29). NOE cross-peaks between G1 and G3 (Figure 7a) indicated continuous stacking between these bases across the bulge (T2). Note that there might be a motion at the bulge as indicated by the broadening of the H8 proton of G3. The structure of a parallel-stranded G-quadruplex of *T30177* with T2 being looped out from the G-tetrad core was recently reported to be stable in a molecular dynamics simulation (38).

Dimeric interface: motion and control of stacking between the monomers

In this section, we describe the nature and stability of the dimeric interface where the stacking between two monomers occurs. Different NMR spectra provided evidence for considerable motion in this region. We observed the broadening of imino protons corresponding to guanines 1, 6, 10 and 14 (Figure 9 and data not shown). Broadening was also observed for some non-exchangeable protons of these residues (Figure 7a). Since all these guanines are located at the dimeric interface, this clearly establishes motion in this region. Possible types of motion include inter-conversion between dimer and monomer or rotation of two subunits about the central axis.

We could remove the stacking between the two G-quadruplex monomers by the addition of two extra thymine bases at the 5′-end (sequence *T30177-TT*, Table 1). Gel electrophoresis experiments (Figure 5) clearly showed the difference between two structures: the monomer (*T30177-TT*) migrated much faster than the dimer

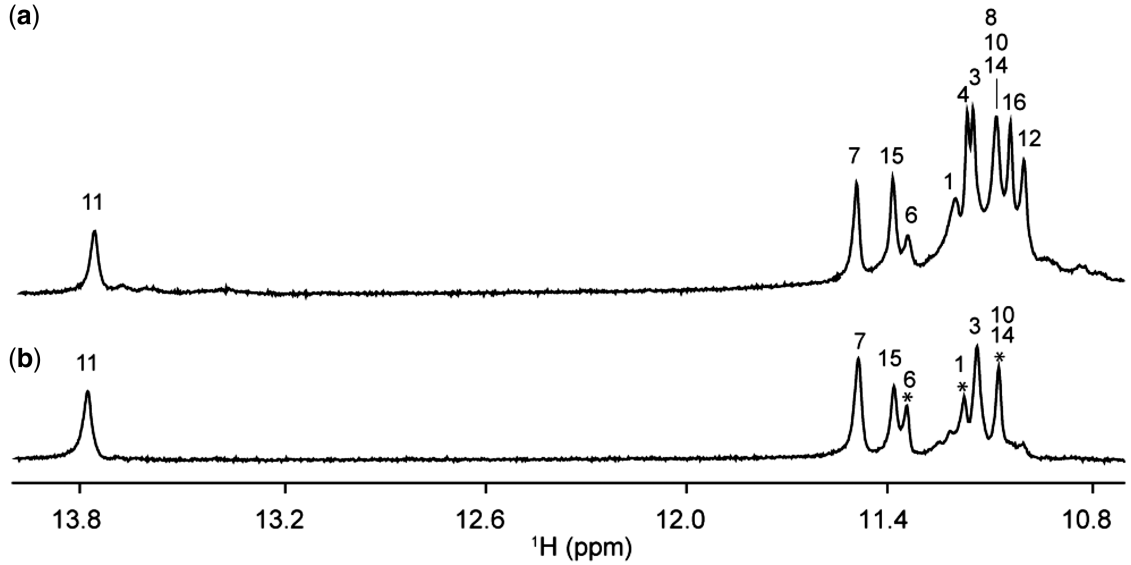

Figure 9. Imino proton spectra of *T30177-I11* (**a**) in H_2O and (**b**) after 13.5 h in ^2H_2O. Imino proton peaks belonging to the central G-tetrad and the G-tetrad at the stacking dimeric interface are protected from the exchange with solvent. Peaks at the interface are labeled with asterisks.

(*T30177* or *T30177-I11*). The monomeric nature of *T30177-TT* and *T30177-I11-TT* were supported by the independence of their melting temperature on the DNA concentration (ranging from 0.5 to 200 μM) (Figure 4b and data not shown). Our unpublished NMR data confirmed that *T30177-TT* forms a monomeric propeller-type parallel-stranded G-quadruplex in this condition.

CONCLUSION

G-rich oligonucleotide *T30177* (or *T30177-I11*) forms a dimeric structure involving two subunits of propeller-type parallel-stranded G-quadruplexes, which are stacked at their 5′-end. All guanines in the sequence participate in G-tetrad formation and there is a bulge of a T residue in each subunit. This work along with other structural studies (39). pointed to the formation of dimeric parallel-stranded G-quadruplexes comprising a total of six G-tetrad layers by various G-rich oligonucleotides that possess HIV-1 integrase inhibition activity.

SUPPLEMENTARY DATA

Supplementary Data are available at NAR Online.

FUNDING

Singapore Ministry of Education grants (ARC30/07 and RG62/07); Singapore Biomedical Research Council (grant 07/1/22/19/542 to A.T.P.). Funding for open access charge: Waived by Oxford University Press.

Conflict of interest statement. None declared.

REFERENCES

1. Davis,J.T. (2004) G-quartets 40 years later: from 5'-GMP to molecular biology and supramolecular chemistry. *Angew. Chem. Int. Ed. Engl.*, **43**, 668–698.
2. Phan,A.T., Kuryavyi,V. and Patel,D.J. (2006) DNA architecture: from G to Z. *Curr. Opin. Struct. Biol.*, **16**, 288–298.
3. Burge,S., Parkinson,G.N., Hazel,P., Todd,A.K. and Neidle,S. (2006) Quadruplex DNA: sequence, topology and structure. *Nucleic Acids Res.*, **34**, 5402–5415.
4. Patel,D.J., Phan,A.T. and Kuryavyi,V. (2007) Human telomere, oncogenic promoter and 5'-UTR G-quadruplexes: diverse higher order DNA and RNA targets for cancer therapeutics. *Nucleic Acids Res.*, **35**, 7429–7455.
5. Neidle,S. (2009) The structures of quadruplex nucleic acids and their drug complexes. *Curr. Opin. Struct. Biol.*, **19**, 239–250.
6. Maizels,N. (2006) Dynamic roles for G4 DNA in the biology of eukaryotic cells. *Nat. Struct. Mol. Biol.*, **13**, 1055–1059.
7. Bates,P.J., Kahlon,J.B., Thomas,S.D., Trent,J.O. and Miller,D.M. (1999) Antiproliferative activity of G-rich oligonucleotides correlates with protein binding. *J. Biol. Chem.*, **274**, 26369–26377.
8. Jing,N., Li,Y., Xiong,W., Sha,W., Jing,L. and Tweardy,D.J. (2004) G-quartet oligonucleotides: a new class of signal transducer and activator of transcription 3 inhibitors that suppresses growth of prostate and breast tumors through induction of apoptosis. *Cancer Res.*, **64**, 6603–6609.
9. Qi,H., Lin,C.-P., Fu,X., Wood,L.M., Liu,A.A., Tsai,Y.-C., Chen,Y., Barbieri,C.M., Pilch,D.S. and Liu,L.F. (2006) G-quadruplexes induce apoptosis in tumor cells. *Cancer Res.*, **66**, 11808–11816.
10. Wyatt,J.R., Vickers,T.A., Roberson,J.L., Buckheit,R.W., Klimkait,T., DeBaets,E., Davis,P.W., Rayner,B., Imbach,J.L. and Ecker,D.J. (1994) Combinatorially selected guanosine-quartet structure is a potent inhibitor of human immunodeficiency virus envelope-mediated cell fusion. *Proc. Natl Acad. Sci. USA*, **91**, 1356–1360.
11. Ojwang,J.O., Buckheit,R.W., Pommier,Y., Mazumder,A., De Vreese,K., Este,J.A., Reymen,D., Pallansch,L.A., Lackman-Smith,C., Wallace,T.L. *et al.* (1995) T30177, an oligonucleotide stabilized by an intramolecular guanosine octet, is a potent inhibitor of laboratory strains and clinical isolates of human immunodeficiency virus type 1. *Antimicrob. Agents Chemother.*, **39**, 2426–2435.
12. Rando,R.F., Ojwang,J., Elbaggari,A., Reyes,G.R., Tinder,R., McGrath,M.S. and Hogan,M.E. (1995) Suppression of human

immunodeficiency virus type 1 activity in vitro by oligonucleotides which form intramolecular tetrads. *J. Biol. Chem.*, **270**, 1754–1760.
13. Mazumder,A., Neamati,N., Ojwang,J.O., Sunder,S., Rando,R.F. and Pommier,Y. (1996) Inhibition of the human immunodeficiency virus type 1 integrase by guanosine quartet structures. *Biochemistry*, **35**, 13762–13771.
14. Jing,N., Rando,R.F., Pommier,Y. and Hogan,M.E. (1997) Ion selective folding of loop domains in a potent anti-HIV oligonucleotide. *Biochemistry*, **36**, 12498–12505.
15. Jing,N.J., Marchand,C., Liu,J., Mitra,R., Hogan,M.E. and Pommier,Y. (2000) Mechanism of inhibition of HIV-1 integrase by G-tetrad-forming oligonucleotides in vitro. *J. Biol. Chem.*, **275**, 21460–21467.
16. de Soultrait,V.R., Lozach,P.Y., Altmeyer,R., Tarrago-Litvak,L., Litvak,S. and Andréola,M.L. (2002) DNA aptamers derived from HIV-1 RNase H inhibitors are strong anti-integrase agents. *J. Mol. Biol.*, **324**, 195–203.
17. Phan,A.T., Kuryavyi,V., Ma,J.B., Faure,A., Andreola,M.L. and Patel,D.J. (2005) An interlocked dimeric parallel-stranded DNA quadruplex: a potent inhibitor of HIV-1 integrase. *Proc. Natl Acad. Sci. USA*, **102**, 634–639.
18. Michalowski,D., Chitima-Matsiga,R., Held,D.M. and Burke,D.H. (2008) Novel bimodular DNA aptamers with guanosine quadruplexes inhibit phylogenetically diverse HIV-1 reverse transcriptases. *Nucleic Acids Res.*, **36**, 7124–7135.
19. Oliviero,G., Amato,J., Borbone,N., D'Errico,S., Galeone,A., Mayol,L., Haider,S., Olubiyi,O., Hoorelbeke,B., Balzarini,J. *et al.* (2010) Tetra-end-linked oligonucleotides forming DNA G-quadruplexes: a new class of aptamers showing anti-HIV activity. *Chem. Commun.*, **46**, 8971–8973.
20. Marchand,C., Maddali,K., Metifiot,M. and Pommier,Y. (2009) HIV-1 IN inhibitors: 2010 update and perspectives. *Curr. Top. Med. Chem.*, **9**, 1016–1037.
21. Gelleert,M., Lipsett,M.N. and Davies,D.R. (1962) Helix formation by guanylic acid. *Proc. Natl Acad. Sci. USA*, **48**, 2013–2018.
22. Pan,B.C., Xiong,Y., Shi,K. and Sundaralingam,M. (2003) Crystal structure of a bulged RNA tetraplex at 1.1 angstrom resolution: Implications for a novel binding site in RNA tetraplex. *Structure*, **11**, 1423–1430.
23. Koizumi,M., Koga,R., Hotoda,H., Momota,K., Ohmine,T., Furukawa,H., Agatsuma,T., Nishigaki,T., Abe,K., Kosaka,T. *et al.* (1997) Biologically active oligodeoxyribonucleotides–IX. Synthesis and anti-HIV-1 activity of hexadeoxyribonucleotides, T GGGAG, bearing 3'- and 5'-end-modification. *Bioorg. Med. Chem.*, **5**, 2235–2243.
24. Urata,H., Kumashiro,T., Kawahata,T., Otake,T. and Akagi,M. (2004) Anti-HIV-1 activity and mode of action of mirror image oligodeoxynucleotide analogue of Zintevir. *Biochem. Biophys. Res. Commun.*, **313**, 55–61.
25. Pedersen,E.B., Nielsen,J.T., Nielsen,C. and Filichev,V.V. (2011) Enhanced anti-HIV-1 activity of G-quadruplexes comprising locked nucleic acids and intercalating nucleic acids. *Nucleic Acids Res.*, **39**, 2470–2481.
26. Craigie,R. (2001) HIV integrase, a brief overview from chemistry to therapeutics. *J. Biol. Chem.*, **276**, 23213–23216.
27. Jing,N., Gao,X., Rando,R.F. and Hogan,M.E. (1997) Potassium-induced loop conformational transition of a potent anti-HIV oligonucleotide. *J. Biomol. Struct. Dyn.*, **15**, 573–585.
28. Li,H., Yuan,G. and Du,D. (2008) Investigation of formation, recognition, stabilization, and conversion of dimeric G-quadruplexes of HIV-1 integrase inhibitors by electrospray ionization mass spectrometry. *J. Am. Soc. Mass. Spectrom.*, **19**, 550–559.
29. Balagurumoorthy,P., Brahmachari,S.K., Mohanty,D., Bansal,M. and Sasisekharan,V. (1992) Hairpin and parallel quartet structures for telomeric sequences. *Nucleic Acids Res.*, **20**, 4061–4067.
30. Smargiasso,N., Rosu,F., Hsia,W., Colson,P., Baker,E.S., Bowers,M.T., De Pauw,E. and Gabelica,V. (2008) G-quadruplex DNA assemblies: Loop length, cation identity, and multimer formation. *J. Am. Chem. Soc.*, **130**, 10208–10216.
31. Phan,A.T., Modi,Y.S. and Patel,D.J. (2004) Propeller-type parallel-stranded G-quadruplexes in the human c-myc promoter. *J. Am. Chem. Soc.*, **126**, 8710–8716.
32. Seenisamy,J., Rezler,E.M., Powell,T.J., Tye,D., Gokhale,V., Joshi,C.S., Siddiqui-Jain,A. and Hurley,L.H. (2004) The dynamic character of the G-quadruplex element in the c-MYC promoter and modification by TMPyP4. *J. Am. Chem. Soc.*, **126**, 8702–8709.
33. Hazel,P., Huppert,J., Balasubramanian,S. and Neidle,S. (2004) Loop-length-dependent folding of G-quadruplexes. *J. Am. Chem. Soc.*, **126**, 16405–16415.
34. Rachwal,P.A., Findlow,I.S., Werner,J.M., Brown,T. and Fox,K.R. (2007) Intramolecular DNA quadruplexes with different arrangements of short and long loops. *Nucleic Acids Res.*, **35**, 4214–4222.
35. Bugaut,A. and Balasubramanian,S. (2008) A sequence-independent study of the influence of short loop lengths on the stability and topology of intramolecular DNA G-quadruplexes. *Biochemistry*, **47**, 689–697.
36. Guédin,A., De Cian,A., Gros,J., Lacroix,L. and Mergny,J.-L. (2008) Sequence effects in single-base loops for quadruplexes. *Biochimie*, **90**, 686–696.
37. Guedin,A., Gros,J., Alberti,P. and Mergny,J.L. (2010) How long is too long? Effects of loop size on G-quadruplex stability. *Nucleic Acids Res.*, **38**, 7858–7868.
38. Li,M.H., Zhou,Y.H., Luo,Q. and Li,Z.S. (2010) The 3D structures of G-Quadruplexes of HIV-1 integrase inhibitors: molecular dynamics simulations in aqueous solution and in the gas phase. *J. Mol. Model.*, **16**, 645–657.
39. Do,N.Q., Lim,K.W., Teo,M.H., Heddi,B. and Phan,A.T. (2011) Stacking of G-quadruplexes: NMR structure of a G-rich oligonucleotide with potential anti-HIV and anticancer activity. *Nucleic Acids Res.* (doi:10.1093/nar/gkr539).
40. Cantor,C.R., Warshaw,M.M. and Shapiro,H. (1970) Oligonucleotide interactions. 3. Circular dichroism studies of the conformation of deoxyoligonucleotides. *Biopolymers*, **9**, 1059–1077.
41. Phan,A.T. and Patel,D.J. (2002) A site-specific low-enrichment (15)N,(13)C isotope-labeling approach to unambiguous NMR spectral assignments in nucleic acids. *J. Am. Chem. Soc.*, **124**, 1160–1161.
42. Huang,X.N., Yu,P.L., LeProust,E. and Gao,X.L. (1997) An efficient and economic site-specific deuteration strategy for NMR studies of homologous oligonucleotide repeat sequences. *Nucleic Acids Res.*, **25**, 4758–4763.
43. Phan,A.T. (2000) Long-range imino proton-13C J-couplings and the through-bond correlation of imino and non-exchangeable protons in unlabeled DNA. *J. Biomol. NMR*, **16**, 175–178.
44. Phan,A.T., Gueron,M. and Leroy,J.L. (2001) Investigation of unusual DNA motifs. *Methods Enzymol.*, **338**, 341–371.
45. Mergny,J.L., Phan,A.T. and Lacroix,L. (1998) Following G-quartet formation by UV-spectroscopy. *FEBS Lett.*, **435**, 74–78.
46. Marky,L.A. and Breslauer,K.J. (1987) Calculating thermodynamic data for transitions of any molecularity from equilibrium melting curves. *Biopolymers*, **26**, 1601–1620.
47. Jin,R.Z., Breslauer,K.J., Jones,R.A. and Gaffney,B.L. (1990) Tetraplex formation of a guanine-containing nonameric DNA fragment. *Science*, **250**, 543–546.
48. Lim,K.W., Lacroix,L., Yue,D.J., Lim,J.K., Lim,J.M. and Phan,A.T. (2010) Coexistence of two distinct G-quadruplex conformations in the hTERT promoter. *J. Am. Chem. Soc.*, **132**, 12331–12342.
49. Smith,F.W. and Feigon,J. (1993) Strand orientation in the DNA quadruplex formed from the Oxytricha telomere repeat oligonucleotide d(G4T4G4) in solution. *Biochemistry*, **32**, 8682–8692.
50. Lim,K.W., Alberti,P., Guedin,A., Lacroix,L., Riou,J.F., Royle,N.J., Mergny,J.L. and Phan,A.T. (2009) Sequence variant (CTAGGG)n in the human telomere favors a G-quadruplex structure containing a G.C.G.C tetrad. *Nucleic Acids Res.*, **37**, 6239–6248.